

Supplementary Material for

Role of polyoxometalate precursors and supports in the selective oxidation of methane into formaldehyde using supported metal oxide subnanocluster catalysts

Keiju Wachi, Tomohiro Yabe^{*}, Takaaki Suzuki, Kentaro Yonesato, Kosuke Suzuki,

Kazuya Yamaguchi^{*}

Department of Applied Chemistry, School of Engineering, The University of Tokyo, 7-3-1 Hongo,
Bunkyo-ku, Tokyo 113-8656, Japan

^{*}E-mail: kyama@appchem.t.u-tokyo.ac.jp; tyabe@g.ecc.u-tokyo.ac.jp

This pdf file includes:

Experimental Methods

Supporting Tables: Table S1–S2

Supporting Figures: Fig. S1–S7

References: S1–S5

Experimental Methods

XAS Measurements. The data reduction procedure for EXAFS consisted briefly of the following steps: pre-edge subtraction, background determination, normalization, and spectra averaging. The edge position is defined to be the first inflexion point on the leading absorption peak. The energy was calibrated using Fe foil for the Fe K-edge XAS. The background in the EXAFS region was approximated using a cubic spline routine and optimized according to the criteria described by Cook and Sayers.^{S1} Then, the spectra were normalized by the edge-step at 50 eV after the absorption edge. The k^3 -weighted EXAFS functions were Fourier transformed, filtered, and fitted in R -space. Fourier filtering was used to isolate the contributions of specific shells and to eliminate low frequency background and high frequency noise. Fourier filtering was done by choosing a window in the Fourier transform spectrum and calculating the inverse Fourier Transform of the selected R -range.

Supporting Tables

Table S1 The iron contents of supported iron catalysts

Catalyst	Fe [wt%]
Fe2/SiO₂	0.17
Fe1/SiO₂	0.16
Fe4/SiO₂	0.63
35Fe2/SiO₂	0.62

Table S2 The list of peaks of observed DRIFTS spectra on SiO₂ and Al₂O₃, and the peak attribution

Wavenumber [cm ⁻¹]		
SiO ₂ , 600 °C	Al ₂ O ₃ , 600 °C	Methanol ^{S2}
3736	3751	3370, $\nu(\text{OH})$
3540	2997	3003, $\nu(\text{CH})$
2959	2906	2977, $\nu(\text{CH})$
2858	1630	2956, $\nu(\text{CH})$
	1572	2921, $\nu(\text{CH})$
		2848, $\nu(\text{CH})$
Formaldehyde ^{S4}	Polyoxymethylene ^{S4}	Carbon monoxide
3430	2980, $\nu(\text{CH}_2)$	2000–2200, $\nu(\text{CO})$
2995	2915, $\nu(\text{CH}_2)$	
2894, $\nu_{\text{as}}(\text{CH}_2)$		
2830, $\nu_{\text{s}}(\text{CH}_2)$		
2732		
1725, $\nu(\text{CO})$		
1717, $\nu(\text{CO})$		
1501, $\delta(\text{CH}_2)$		
Methoxide ^{S3}	Dioxymethylene ^{S4}	Formate ^{S4}
2928, $\nu_{\text{as}}(\text{OH})$	2950–2970, $\nu_{\text{as}}(\text{CH}_2)$	2970, $\nu_{\text{as}}(\text{OCO}) + \delta(\text{CH})$
2832, $\nu_{\text{s}}(\text{CH})$	2840–2870, $\nu_{\text{s}}(\text{CH}_2)$	2905, $\nu(\text{CH})$
	2750–2765, $2\nu_{\text{w}}(\text{CH}_2)$	2750, $\nu_{\text{s}}(\text{OCO}) + \delta(\text{CH})$
		1595, $\nu_{\text{as}}(\text{OCO})$

Detailed explanation for *in situ* DRIFTS spectra. For the DRIFTS spectrum of Al₂O₃, the adsorbed species was determined to be formate because the peaks at 2997, 2907, and 1572 cm⁻¹ were consistent with those of formate ions adsorbed on Al₂O₃. In the case of the DRIFTS spectrum of SiO₂, the adsorbed species corresponding to 2959 and 2858 cm⁻¹ were determined through a process of elimination. Seven possible adsorbed species and their reported attributions were presented in Table S2. Firstly, formaldehyde, formate, and carbon monoxide were eliminated due to the absence of peaks in the range of 1500–2500 cm⁻¹, where their characteristic peaks derived from $\nu(\text{CO})$, $\nu_{\text{as}}(\text{OCO})$, or $\nu(\text{CO})$ appeared. Subsequently, polyoxymethylene and methoxide were excluded because there were no specific peaks consistent with the observed peaks. Finally, methanol was eliminated for two reasons: the absence of the peak derived from $\nu(\text{OH})$ around 3370 cm⁻¹, and the assumption that methanol would hardly remain on SiO₂ at 600 °C under vacuum. Consequently, we concluded that the remaining species, dioxymethylene, could be attributed to the peaks at 2959 and 2858 cm⁻¹.

Supporting Figures

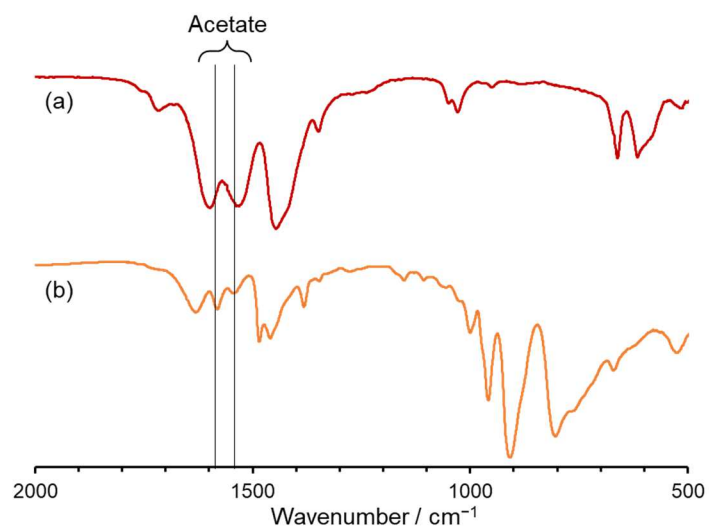


Fig. S1 IR spectra of (a) $\text{Fe}_3\text{O}(\text{CH}_3\text{CO}_2)_7(\text{H}_2\text{O})$ and (b) **Fe4**.

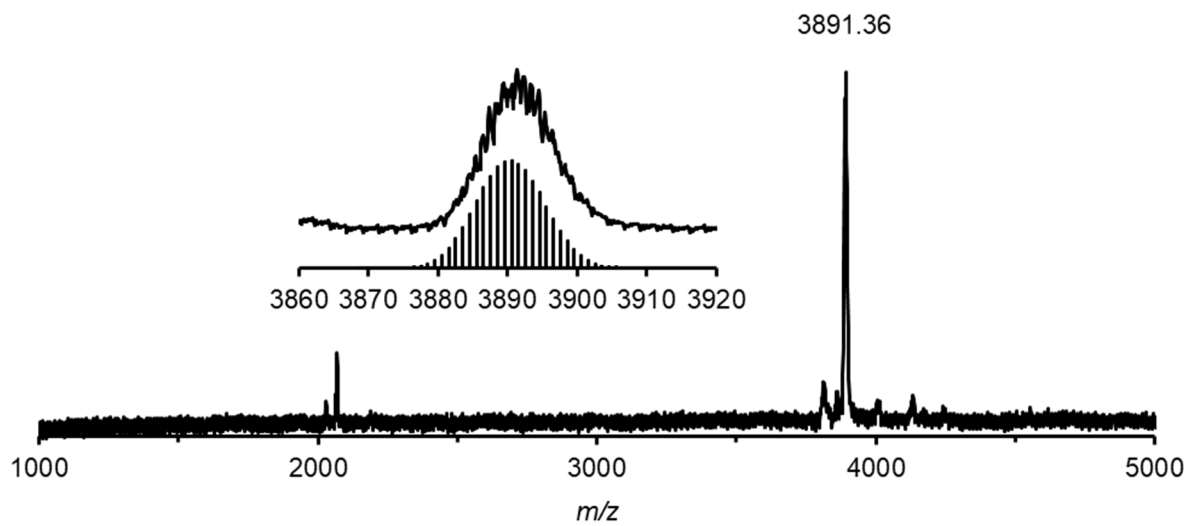


Fig. S2 Positive-ion CSI-mass spectrum of Fe₄ in acetonitrile. Inset: spectrum in the range of m/z 3860–3920, and a simulated pattern for [TBA₅Fe₄(OH)₃(CH₃CO₂)₃SiW₉O₃₄]⁺ (theoretical m/z : 3890.48).

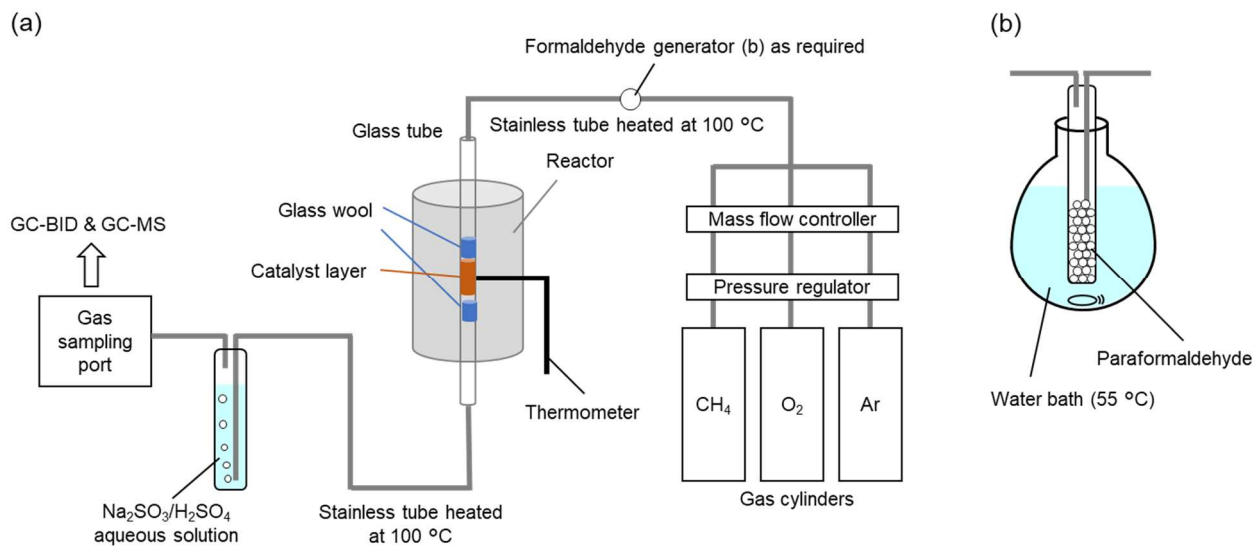


Fig. S3 Schematic image of an experimental apparatus: (a) overall image and (b) formaldehyde generator.

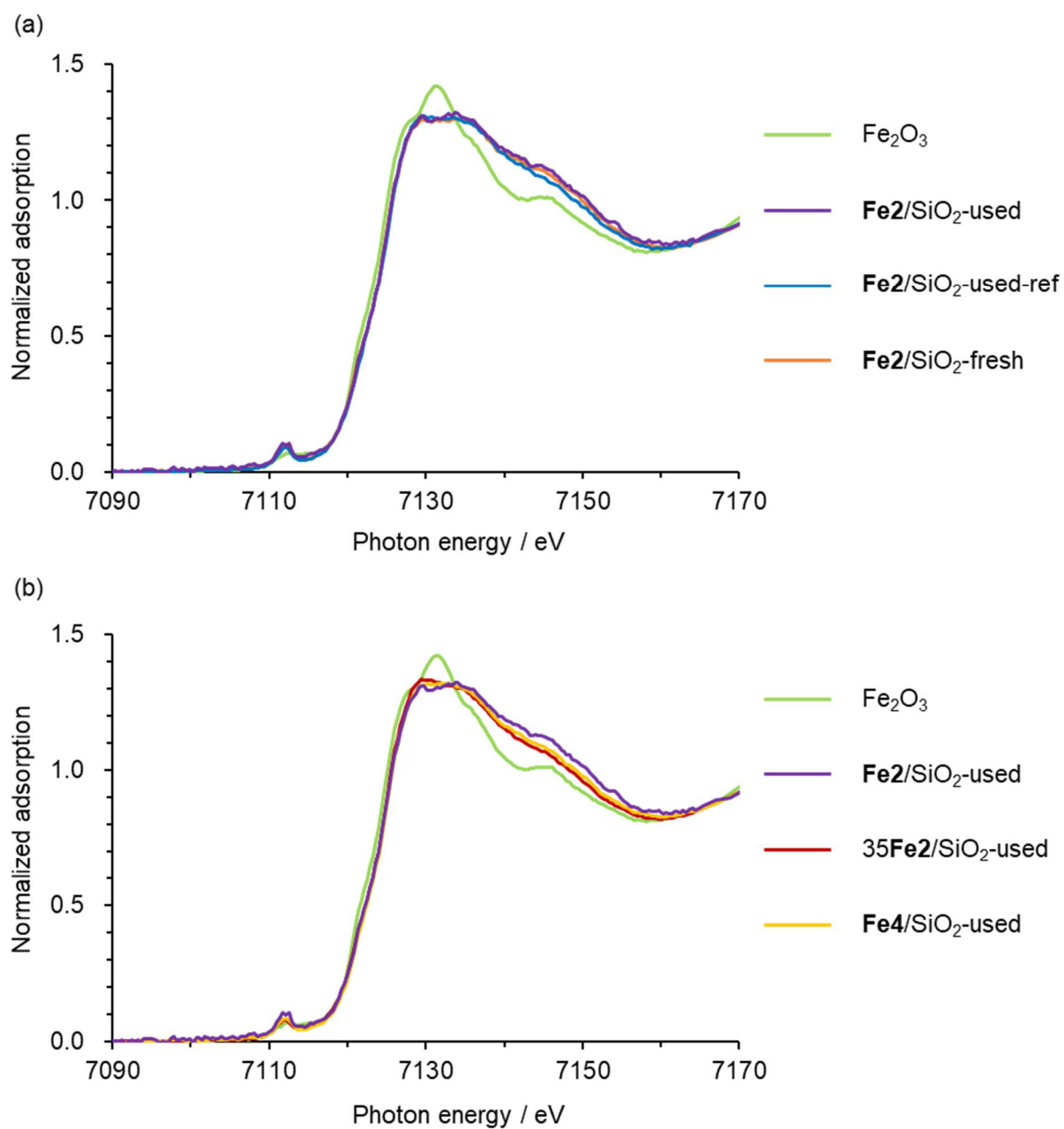


Fig. S4 Fe K-edge XANES spectra of various catalysts before and after the reaction. The reaction conditions were indicated in Table 1. The Fe K-edge XANES spectrum of **Fe2/SiO₂-used-ref** was the same as previously reported.^{S5}

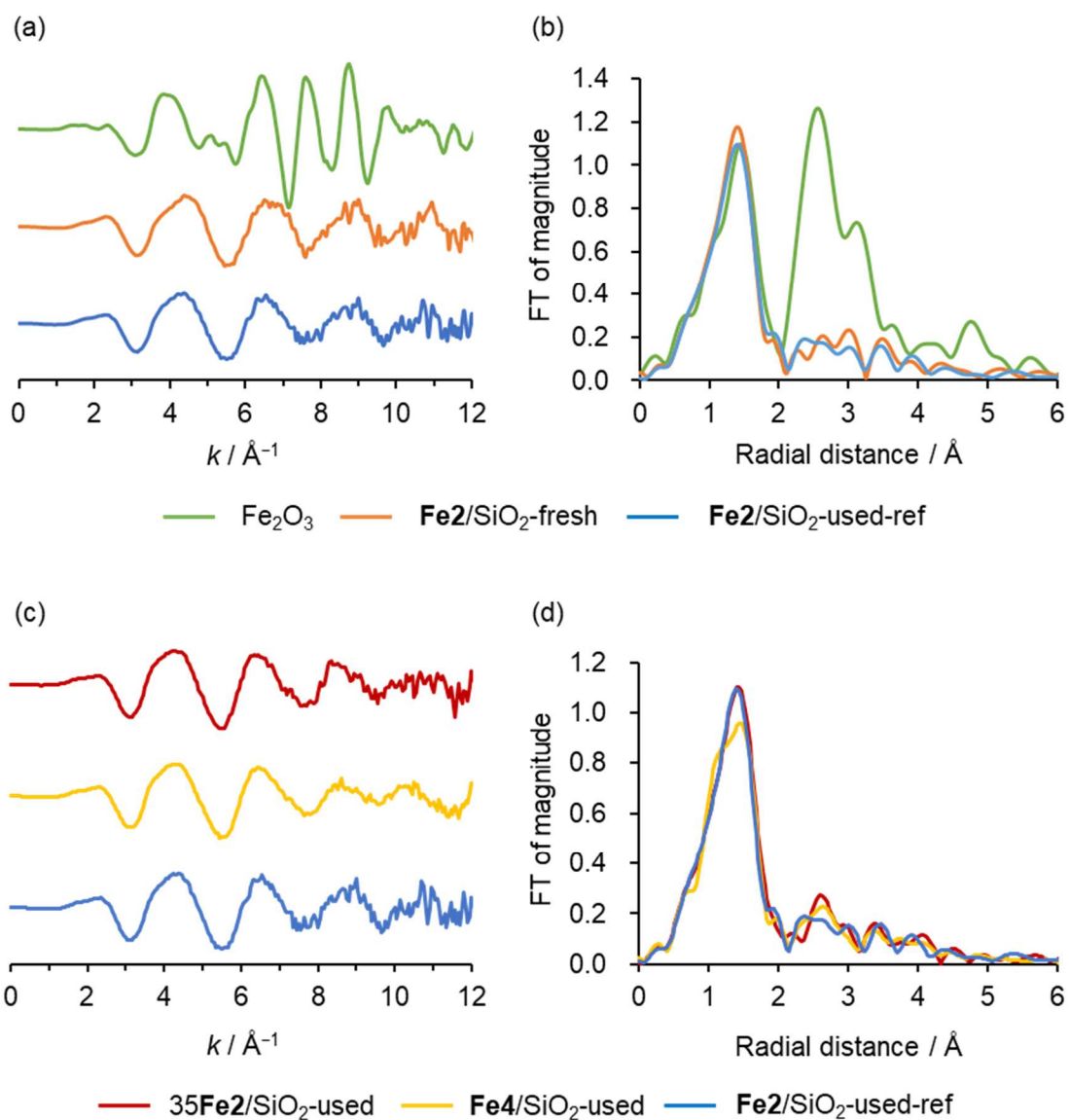


Fig. S5 k^3 -weighted (a) Fe K-edge EXAFS oscillation and (b) Fourier-transformed Fe K-edge EXAFS spectra ($k = 3\text{--}12 \text{\AA}^{-1}$) of Fe_2/SiO_2 before and after the reaction. The Fe K-edge EXAFS spectra of Fe_2/SiO_2 -used-ref were shown in the previous paper.^{S5} (c) Fe K-edge EXAFS oscillation and (d) Fourier-transformed Fe K-edge EXAFS spectra ($k = 3\text{--}12 \text{\AA}^{-1}$) of $^{35}\text{Fe}_2/\text{SiO}_2$ and Fe_4/SiO_2 catalysts after the reaction.

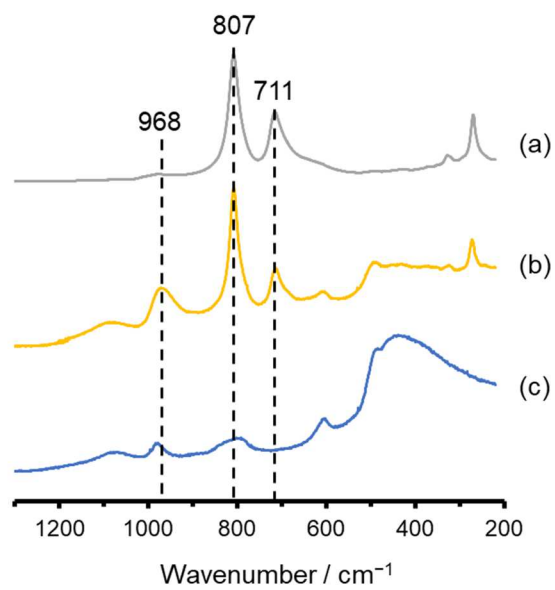


Fig. S6 Raman spectra of (a) **Fe4**/SiO₂-used, (b) **Fe2**/SiO₂-used, and (c) SiO₂.

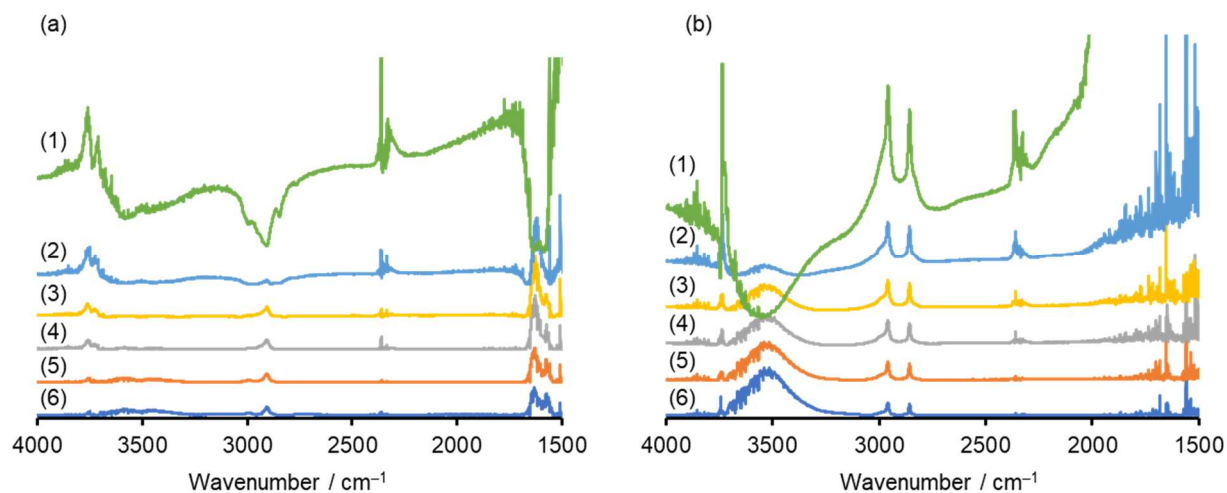


Fig. S7 Time variation of *in situ* DRIFTS spectra of (a) Al_2O_3 and (b) SiO_2 . Analytic conditions: 600 °C, Gas: N_2 (20 mL min^{-1}) + HCHO (generated from paraformaldehyde at 55 °C). (1) 60 min after HCHO/ N_2 flow; (2) *in vacuo*, 0 min; (3) *in vacuo*, 5 min; (4) *in vacuo*, 10 min; (5) *in vacuo*, 30 min; (6) *in vacuo*, 60 min. The absorbance intensities on the vertical axis are Kubelka–Munk-transformed.

Reference:

- S1 J.W. Cook Jr. and D.E. Sayers, *J. Appl. Phys.*, 1981, **52**, 5024–5031.
- S2 D. B. Clarke, D. K. Lee, M. J. Sandoval and A. T. Bell, *J. Catal.*, 1994, **150**, 81–93.
- S3 S. Kattel, B. Yan, Y. Yang, J. G. Chen and P. Liu, *J. Am. Chem. Soc.*, 2016, **138**, 12440–12450.
- S4 G. Busca, J. Lamotte, J.-C. Lavalley and V. Lorenzelli, *J. Am. Chem. Soc.*, 1987, **109**, 5197–5202.
- S5 K. Wachi, T. Yabe, T. Suzuki, K. Yonesato, K. Suzuki and K. Yamaguchi, *Appl. Catal. B*, 2022, **314**, 121420.